COMMUNICATION

Slight mistuning of a cryogenic probe significantly perturbs the water ^{1}H precession frequency

Dennis A. Torchia

Abstract A shift of the water proton precession frequency is described that can introduce errors in chemical shifts derived using the water signal as the chemical shift reference. This shift, f_s, arises as a consequence of radiation damping when the water proton and detector circuit resonance frequencies differ. Herein it is shown that experimental values of f_s, measured as a function of detector circuit tuning offset for 500 and 900 MHz cryogenic probes, are in good agreement with theory. Of importance is the fact that even a small degree of mistuning, which does not significantly impact the performance of a pulse sequence, introduces chemical shift errors of ± 0.03 ppm, that negatively impact many types of experiments. A simple remedy that attenuates the frequency shift is presented.

Keywords Probe · Tuning · Water · Proton · Precession · Frequency · Chemical shift · Reference

Abbreviations
RD   Radiation damping
TSP   Trimethylsilylpropionic acid-d4, sodium salt

Most biomolecular NMR studies are carried out in aqueous solvents, where the water resonance serves as a useful and common chemical shift reference. Because of the high concentration and large magnetogyric ratio of the water protons, a large water proton magnetization precesses around the external field, B_o, following an RF pulse, and

D. A. Torchia (✉)
National Institute of Dental and Craniofacial Research, National Institutes of Health, Bethesda, MD 20892-4307, USA
e-mail: dtorchia@mail.nih.gov

induces a significant current, I, in the probe coil, particularly when experiments are carried out at high field strength with high-Q probes. As current flows through the coil resistance, R, I^2R power is dissipated as heat. Because the energy lost must be supplied by the spin system, the water magnetization vector rotates from the transverse plane towards B_o. This phenomenon, called radiation damping, RD, was first analyzed quantitatively by Bloembergen and Pound (1954). A widely-observed consequence of RD is the decay of transverse water magnetization, with the concomitant growth in M_z, at a rate far in excess of that due to spin relaxation. RD can therefore cause substantial broadening of the water signal, reducing the accuracy with which the water chemical shift can be measured. If necessary, this problem can be overcome by saturating the water magnetization (e.g. by applying a train of 120° pulses (Markley et al. 1971) followed by a short delay) before recording a spectrum. This significantly reduces the magnitude of the precessing water magnetization and thereby attenuates RD.

A more subtle, and potentially more pernicious, effect of RD is a shift of the ^{1}H water precession frequency that occurs when the resonance frequency of the probe detection circuit, f_{LC}, differs from the unperturbed resonance frequency of the water protons, f_o (Vlassenbroek et al. 1995). Vlassenbroek et al. (1995) showed that, in this circumstance, the precession frequency of the water protons is time dependent, with the precession frequency of the water signal shifted by an amount given by

$$f_s = (xQ/\pi\tau)M_z(t)/M_o \tag{1}$$

where,

$$x = (f_o - f_{LC})/f_o \tag{2}$$

Equation 1 follows from a more general result (Vlassenbroek et al. 1995) and is accurate when $|x| \ll 1$.

In Eqs. 1 and 2, f_s is the predicted frequency shift (in Hz), Q is the quality factor of the probe detection circuit, τ is the RD time constant, $M_z(t)$ is the z magnetization after application of an RF pulse, M_o is the magnitude of the equilibrium magnetization. To a good approximation f_s is time independent when M_o is nutated by an RF pulse through a small angle ($\approx 30°$ or less) so that $M_z(t) \cong M_o$, yielding the simple, time independent, result

$$f_s \approx (xQ/\pi\tau) \tag{3}$$

Note that, unless $x = 0$, a frequency shift is predicted whose magnitude and sign depend upon x.

Experiments were recorded to measure f_s on Bruker Avance 500 and 900 NMR spectrometers, each equipped with a cryogenic probe, and operating with the carrier frequency, f_c, set at 499.53 and at 900.274 MHz, respectively. The sample consisted of a 5 mm OD tube containing ca. 1% trimethylsilylpropionic acid-d4, sodium salt (TSP) dissolved in ca. 95% H_2O/5% D_2O. Initially, the transmitter circuit of each probe was tuned by adjusting the variable capacitors so that the reflected power was minimized at f_c using the Bruker WOBB function. Following application of an RF pulse (nutation angle ca. 35° and 3° at 499.53 and 900.274 MHz, respectively) the FID was recorded and Fourier transformed, and the external field was then adjusted so that the water resonance frequency, f_o, was equal to f_c. Subsequent spectra were recorded using f_{LC} in the range -250 kHz $< f_o - f_{LC} < 250$ kHz at $f_c = 499.53$ MHz and -1250 kHz $< f_o - f_{LC} < 1250$ kHz at $f_c = 900.274$ MHz.

It is noteworthy that, when the transmitter resonance frequency equaled the resonance frequency of water ($f_o = 900.274$ MHz), the linewidth of the water signal was *not* maximal. This observation implies that the transmitter and detector circuit optimal tuning (resonance) frequencies are different on the 900 MHz instrument. At 500 MHz, the resonance frequencies of transmitter and detector circuits were found to be the same, within measurement error. In this paper, f_{LC} denotes the resonance frequency of the detector circuit, not that of the transmitter circuit indicated by the WOBB function.

The TSP resonance frequency did not change as f_{LC} was varied (data not shown). In contrast, as seen in Figs. 1 and 2, the water resonance frequency shift, f_s, is significant and is a sensitive function of f_{LC}. The quantitative comparison of the measured values of f_s with those predicted by Eq. 3 was facilitated by measuring the linewidth of the water signal, Γ_w, at each value of f_{LC}. Because the nutation angle is small, to a good approximation, $1/\pi\tau$ in Eq. 3 can be replaced by Γ_w (Vlassenbroek et al. 1995), yielding

$$f_s = \Gamma_w xQ. \tag{4}$$

Note that, when Γ_w and x are known from experiment, f_s depends upon a single unknown constant, Q, the circuit
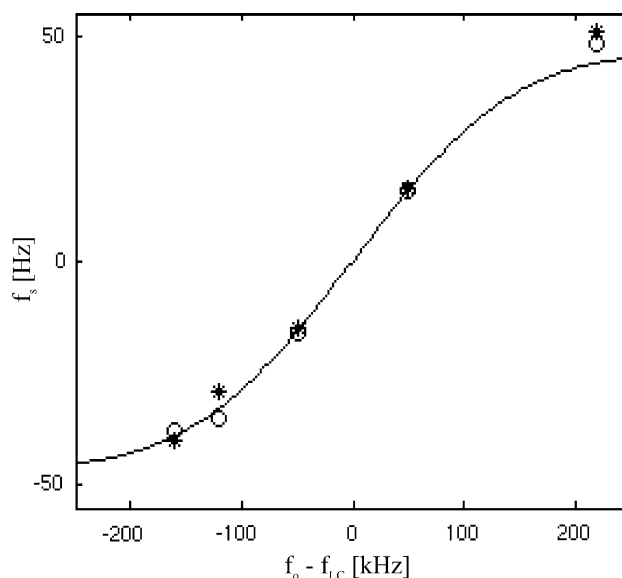
Fig. 1 Comparison of measured values of f_s (*) at 500 MHz with those predicted by Eq. 4, *open circles*, and by Eq. 6, *solid line*. The frequency shifts are plotted as a function of $f_o - f_{LC}$, the difference between the resonance frequency of water and the resonance frequency of the probe detection circuit. Spectra were recorded using a single RF pulse, ca. 35° nutation, for values of $f_o - f_{LC}$ equal to $-160, -120, -50, 50, 220$ kHz. At each of these values of $f_o - f_{LC}$, f_s was calculated with $1/\pi\tau$ set equal to the observed value of the respective water linewidth, $\Gamma_w = 130, 160, 175, 173, 120$ Hz. A value of Q = 910 was obtained using Eq. 4 and the above values of Γ_w to best fit (*open circles*) the measured values f_s. Because the resonance frequencies of the transmitter and detection circuits were the same, f_{LC} was taken as the frequency at which the instrument WOBB function displayed its minimum value. In fitting the frequency shift data, f_s was set to zero when $f_{LC} = f_o$. The rms difference between measured and calculated values of f_s was 3.1 Hz. A value of Q = 893 was obtained using Eq. 6 and $\Gamma_{wo} = 181$ Hz (the water linewidth when $f_o = f_{LC}$) to best fit (*solid line*) the measured values of f_s. The rms difference between measured and calculated values of f_s was 3.6 Hz

quality factor. This quantity was estimated by fitting Eq. 4 to the 500 MHz experimental data, Fig. 1. The values of f_s, shown as open circles in Fig. 1, were calculated using the best-fitted value of Q = 910. This large value of Q is a consequence of the low coil resistance of the cryogenic probe.

An alternative approach to fit the data is afforded by utilizing the theoretical relationship between τ and the circuit impedance, Z,

$$\tau = \tau_o |Z^2|/R^2 = \tau_o(1 + 4x^2Q^2) \tag{5}$$

where Z is the impedance at f_o for arbitrary f_{LC}, and R and τ_o are the respective impedance and RD time constant when $f_{LC} = f_o$. Substituting the above expression for τ in Eq. 3, and replacing $(1/\pi\tau_o)$ by Γ_{wo}, the water linewidth when $f_{LC} = f_o$, Eq. 3 becomes

$$f_s = \Gamma_{wo} xQ/(1 + 4x^2Q^2) \tag{6}$$

Note that Eq. 6 predicts that although f_s is proportional to x when $|x|Q \ll 1$, it approaches zero as $|x|Q$ increases. The latter result is expected on physical grounds because, as the circuit impedance increases, the current in the coil decreases and the power dissipated decreases in proportion to the square of the current. Using Eq. 6 to best fit the values of f_s measured at 500 MHz, we obtain $Q = 893$, in reasonable agreement with Q obtained using Eq. 6.

As seen in Fig. 2, significant frequency shifts are also observed at 900 MHz. The more extensive data acquired at 900 MHz are well fitted by both Eqs. 4 and 6, and clearly show the reduction in $|f_s|$ predicted by theory for large tuning offsets. Moreover, the data verify that $\max|f_s| = \Gamma_{wo}/4$ when $f_o - f_{LC} = \pm f_o/2Q$, as predicted by Eq. 6. Fitting the large number of data points that were acquired at
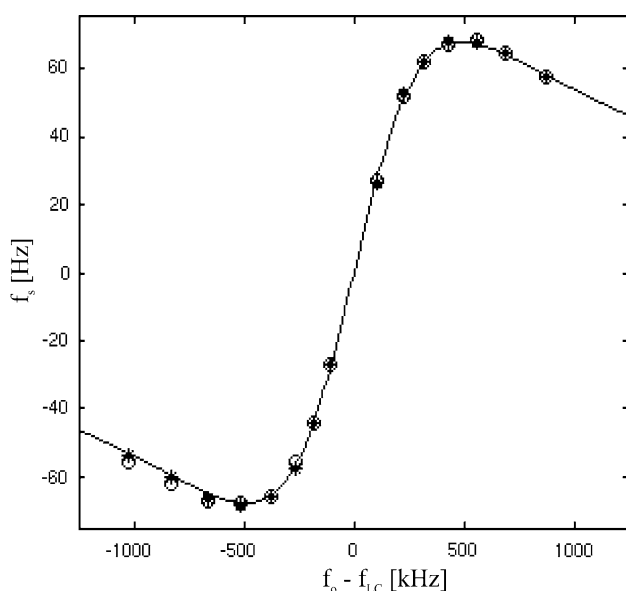
Fig. 2 Comparison of measured values of f_s (*) at 900 MHz with those predicted by Eq. 4, *open circles*, and by Eq. 6, *solid line*. The frequency shifts are plotted as a function of $f_o - f_{LC}$, the difference between the resonance frequency of water and the resonance frequency of the probe detection circuit. Spectra were recorded using a single RF pulse, ca. 3° nutation, for values of $f_o - f_{LC}$ in the range of ca. ± 1 MHz. Because the values of transmitter and detector resonance frequencies differed, values of both Q and f_{LC} were determined using Eq. 4 to fit the data, while values of Q, f_{LC}, and Γ_{wo} were determined using Eq. 6 to fit the data. The best fits using both equations (rms <1 Hz) were obtained using a detector resonance frequency that was 267 kHz larger than that of the transmitter, which corresponded to values of $f_o - f_{LC}$ of -1023, -833, -663, -513, -373, -263, -181, -102, 102, 227, 317, 427, 557, 687, 877 kHz. At each value of $f_o - f_{LC}$, the respective observed water linewidth, $\Gamma_w = 54$, 73, 100, 131, 175, 210, 241, 260, 261, 225, 193, 155, 121, 93, 65 Hz, was used to best fit the data with Eq. 4, which yielded $Q = 910$. The rms difference between measured and calculated values of f_s was 0.9 Hz. A value of $Q = 912$ and $\Gamma_{wo} = 271$ Hz (the water linewidth when $f_o = f_{LC}$) was obtained using Eq. 6 to best fit (*solid line*) the measured values of f_s. The rms difference between measured and calculated values of f_s was 0.9 Hz

900 MHz, yielded both the difference between transmitter and detector resonance frequencies (267 kHz), as well as the Q of the detector circuit, Fig. 2. It is interesting that the best-fitted values of Q at 900 MHz (ca. 910) are approximately equal to the Q values obtained at 500 MHz (ca. 900). In a circuit in which the coil resistance is the primary source of loss, Q is expected to be proportional to $\sqrt{(\gamma B_o)}$ (Hoult and Richards 1976). Presumably other sources of loss, such as those arising from the ionic and dielectric conductivity of the solution (Horiuchi et al. 2005), are significant and increase as frequency increases, thereby attenuating the expected increase in Q.

Perhaps the most interesting feature revealed by both figures is that mistuning the probe detector circuit by only ca. 0.01% of the carrier frequency (50 or 100 kHz at 500 or 900 MHz, respectively) leads to changes in the water resonance frequency of ± 0.03 ppm. Therefore, proton chemical shifts of two spectra, referenced to water, could suffer a difference of 0.06 ppm solely as a consequence of small fractional differences (positive or negative) between f_{LC} and f_o. Such an error in chemical shift referencing would negatively impact many types of NMR experiments, in particular those that measure, $\Delta\delta$'s, the small residual anisotropic chemical shifts (Cornilescu and Bax 2000) which provide useful restraints for determining the structures of proteins (Vallurupalli et al. 2008) and nucleic acids (Grishaev et al. 2006; Hansen and Al-Hashimi 2006). Also the accuracy of programs that automate NOE and shift assignments strongly depends upon correct chemical shift referencing (Herrmann et al. 2002; Huang et al. 2005; Fiorito et al. 2008).

Of related interest is the fact that slightly mistuning the detector circuit increases the magnitude of its impedance by the factor ca. $1 + 2x^2Q^2$ (when $4x^2Q^2 \ll 1$, see Eq. 5), whose value equals 1.02 when $|f_o - f_{LC}|/f_o = 0.01\%$ and $Q = 900$. Therefore the slight mistuning decreases the intensity of RF pulses and NMR signals by only a few percent, which does not perceptibly impact the performance of a pulse sequence. At the same time, as shown above, this small degree of circuit mistuning can cause significant variations in values of chemical shifts derived using a water reference. In order for the water signal to serve as an accurate chemical shift reference, a cryogenic probe should be carefully tuned and the water magnetization saturated by a long series of pulses (Markley et al. 1971) followed by a short delay (e.g. 100 ms) prior to application of an observe pulse.

As noted by Edzes (1990) and Vlassenbroek et al. (1995), the dipolar field also modulates and shifts the water proton precession frequency. As is the case with RD, the frequency shift is proportional to M_z; however it does not depend upon the circuit tuning and is the same for all spins in the sample. Therefore, no error in chemical shift referencing arises from the dipolar field.

References

Bloembergen N, Pound RV (1954) Radiation damping in magnetic resonance experiments. Phys Rev 95:8–12

Cornilescu G, Bax A (2000) Measurement of proton, nitrogen, and carbonyl chemical shielding anisotropies in a protein dissolved in a dilute liquid crystalline phase. J Am Chem Soc 122:10143–10154

Edzes HT (1990) The nuclear magnetization as the origin of transient changes in the magnetic-field in pulsed NMR experiments. J Magn Reson 86:293–303

Fiorito F, Herrmann T, Damberger FF, Wüthrich K (2008) Automated amino acid side-chain NMR assignment of proteins using 13C- and 15N-resolved 3D [1H, 1H]-NOESY. J Biomol NMR 42:23–33

Grishaev A, Ying JF, Bax A (2006) Pseudo-CSA restraints for NMR refinement of nucleic acid structure. J Am Chem Soc 128:10010–10011

Hansen AL, Al-Hashimi HM (2006) Insight into the CSA tensors of nucleobase carbons in RNA polynucleotides from solution measurements of residual CSA: towards new long-range orientational constraints. J Magn Reson 179:299–307

Herrmann T, Güntert P, Wüthrich K (2002) Protein NMR structure determination with automated NOE assignment using the new software CANDID and the torsion angle dynamics algorithm DYANA. J Mol Biol 319:209–227

Horiuchi T, Takahashi M, Kikuchi J, Yokoyama S, Maeda H (2005) Effect of dielectric properties of solvents on the quality factor for a beyond 900 MHz cryogenic probe model. J Magn Reson 174:34–42

Hoult DJ, Richards RE (1976) The signal-to-noise ratio of the nuclear magnetic resonance experiment. J Magn Reson 24:71–85

Huang JY, Moseley HNB, Baran MC, Arrowsmith C, Powers R, Tejero R, Szyperski T, Montelione GT (2005) An integrated platform for automated analysis of protein NMR structures. Meth Enzymol 394:111–135

Markley JL, Horsley WJ, Klein MP (1971) Spin-lattice relaxation measurements in slowly relaxing complex spectra. J Chem Phys 55:3604–3605

Vallurupalli P, Hansen DF, Kay LE (2008) Probing structure in invisible protein states with anisotropic NMR chemical shifts. J Am Chem Soc 130:2734–2735

Vlassenbroek A, Jeener J, Broekaert P (1995) Radiation damping in high resolution liquid NMR: a simulation study. J Chem Phys 103:5886–5897